Desalination and Water Treatment
www.deswater.com
doi: 10.1080/19443994.2013.806223

52 (2014) 5175–5186
August

Taylor & Francis
Taylor & Francis Group

Fennel seed extract as green corrosion inhibitor for 304 stainless steel in hydrochloric acid solutions

A.S. Fouda[a,*], S.M. Rashwan[b], H.A. Abo-Mosallam[c]

[a]*Faculty of Science, Department of Chemistry, El-Mansoura University, El-Mansoura 35516, Egypt*
Tel. +2 050 2365730; Fax: +2 050 2446254; email: asfouda@mans.edu.eg
[b]*Faculty of Science, Department of Chemistry, Suez Canal University, Ismaïlia, Egypt*
[c]*Water and Waste Water Company, Dakahlia, Egypt*

Received 25 January 2013; Accepted 7 May 2013

ABSTRACT

The inhibitive and adsorptive characteristics of ethanol extract of fennel seeds for the corrosion of 304 stainless steel (SS) in 1 M HCl solutions have been studied using weight loss, potentiodynamic polarization, electrochemical impedance spectroscopy, and electrochemical frequency modulation methods for monitoring corrosion. Ethanol extract of fennel is a good adsorption inhibitor for the corrosion of 304 SS in HCl. The inhibitive property of the extract is attributed to the presence of anethol and fenchone as major constituents in the extract. Inhibition efficiency increased with increasing concentration of the extract but decreased by increasing the temperature. Adsorption studies revealed that Langmuir adsorption isotherm is the best adsorption model applicable to the adsorption of fennel extract on 304 SS surface. Activation and adsorption parameters were evaluated and discussed. Potentiodynamic polarization measurements indicated that the inhibitor is of mixed type. The results obtained from these techniques were in good agreement to prove the validity of these tools in the measurements of the tested inhibitor.

Keywords: Corrosion; Fennel; 304 SS; HCl; Green inhibitor

1. Introduction

Industrial processes such as acid pickling, acid cleaning, and etching, often involve contact between steel and an acidic medium which implies that the use of inhibitors is necessary [1–3]. Most corrosion inhibitors are either synthesized from cheap raw materials or are chosen from organic compounds containing electronegative functional groups and π-electrons in triple or conjugated double bonds. The presence of aromatic rings and hetero atoms (such as S, N, O, and P) are the major adsorption centers for these inhibitors [4–6]. It has been found that the level of protection of organic corrosion inhibitors depends on the nature of the adsorption of the inhibitor on the metal surface, the mode of adsorption, chemical structure of the inhibitor, the type of the aggressive solution, etc. [7,8].

There are several studies on the application of plant extracts [9], as well as other organic inhibitors [10–16] against corrosion of steel in acidic fluids. Loto had reported the application of the extract of *Mangifera indica* leaves and bark for corrosion of mild

---

*Corresponding author.

steel in diluted sulfuric acid (H_2SO_4) medium [17,18]. The inhibitive effect of *Zenthoxylum alatum* fruit extract was reported for corrosion of mild steel in phosphoric acid medium at temperatures ranging from 50 to 80°C [19]. Satapathy et al. studied the methanol extract of *Justicia gendarussa* leaves for corrosion inhibition of mild steel in HCl solution [20]. The inhibitive action of leaves, seeds, and a combination of leaves and seeds of *Phyllanthus amarus* was reported by Okafor et al. for corrosion of mild steel in HCl and H_2SO_4 [21]. Pennyroyal oil was extracted from *Mentha pulegium* and studied for corrosion inhibition of steel in HCl corrosive medium [22]. The major constituent of Pennyroyal oil was *R*-(+)- pulegone [23]. According to Riggs [24], if the displacement of corrosion potential during electrochemical polarization of the metal is more than ±85 mV with respect to the corrosion potential of the blank, the inhibitor can be considered as a distinctive cathodic or anodic type. Similarly, inhibition effect of Jojoba oil and Artemisia oil were studied for steel corrosion in HCl medium under different temperatures [25,26]. Sethuraman et al. have performed a series of investigations on corrosion inhibition of mild steel in acidic medium using various plant extracts. For example, black pepper [27], Datura metal [28], and *Strychnos nux-vomica* [29] has been studied against the corrosion of mild steel in HCl as well in H_2SO_4. The extract of khillah seeds (*Ammi visnaga*) was studied against the corrosion of SX 316 stainless steel (SS) in HCl solution [30]. The anticorrosion behavior of lupine (*Lupinous albus*) extract on the corrosion of steel in aqueous solution of H_2SO_4 and HCl was investigated by Abdel-Gaber et al. [31]. The inhibitor showed comparatively higher efficiency in HCl than in H_2SO_4. The leaf extract showed significantly higher inhibition efficiency (IE) (97%) than the seed extract (94%). In a similar manner, the extracts of Carica papaya leaves, seeds, heartwood, and bark were evaluated for corrosion inhibition of mild steel in H_2SO_4 acid solution [32]. The leaf extract showed higher IE compared with the extracts from seed, heartwood, and bark. El-Etre evaluated the inhibition potential of the aqueous extract of zallouh root for corrosion of carbon steel in HCl solution [33].

The aim of this work is to study the effect of using extract of Fennel as green inhibitor for the corrosion of 304 SS in HCl solutions using weight loss method (chemical method) and electrochemical techniques (potentiodynamic polarization method, electrochemical impedance spectroscopy (EIS) method, and electrochemical frequency modulation (EFM) method).

2. Experimental

2.1. Materials

The experiments were performed with SS type 304 specimens in the form of rods and sheets with the following composition (wt.%): 18 Cr, 8 Ni, less than 0.03 C, and the remainder iron. For electrochemical measurements, the sheets were welded with Cu-wire for electrical connection and mounted onto glass tubes of appropriate diameter using Araldite to offer an active surface of 1 cm^2 geometric area to contact the test solution. Prior to each experiment, these sheets were abraded with emery paper (400–1,000 grade) and degreased with trichloroethylene, washed with bidistilled water and then dried. Electrochemical polarization experiments were carried out in a conventional three-electrode cell with a capacity of 100 ml. A platinum counter electrode (1 cm^2) and a saturated calomel electrode (SCE) were coupled to a fine Luggin capillary as the reference electrode to minimize the ohmic contribution. The Luggin capillary was kept close to the working electrode. HCl (37%) was of analytical grade and bidistilled water was used for all preparations. All experiments were carried out open to the atmosphere. The experiments were repeated and the reproducibility was tested and confirmed.

2.2. Fennel extract

The analysis of fennel seeds extract, obtained by hydrodistillation, using Gas Chromatography (GC) and Gas Chromatography/Mass Spectrometry (GC/MS) showed that the major components were Anethol (50–60%) and Fenchone (18–22%) [34]. Interestingly, the composition of fennel oil was variable according to the area of harvest and the stage of development. The analysis allowed the identification of 21 components which accounted for 96.6% of the total weight. The molecular structure of Anethol and Fenchone are shown in Fig. 1.

2.3. Weight loss method

The samples measuring $2 \times 2 \times 0.2$ cm were prepared as before. The specimens were immersed in 250 ml beaker, which contained 100 ml of 1 M HCl with and without different concentrations of inhibitors. After 3 h, the specimens were taken out, washed, dried, and weighed accurately. The average weight loss of the parallel SS sheets could be obtained. Then, the tests were carried out at a temperature range of 25–45°C. The IE of the inhibitor and corrosion rate

Chemical Constituents	Structure	IUPAC
Anethol	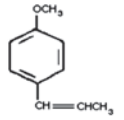	1-methoxy-4-(1-propenyl) benzene
Fenchone	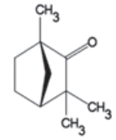	1,3,3-Trimethylbicyclo[2.2.1]heptan-2-one

Fig. 1. Molecular structures and names of main components in fennel seeds extract.

(CR) in mg cm^{-2} min^{-1} of SS type 304 in HCl solution were calculated using Eqs. (1) and (2), respectively [35]:

$$\% \text{ IE} = [1 - (W_1/W_2)] \times 100 \quad (1)$$

$$\text{CR} = [W_1 - W_2)]/At \quad (2)$$

where W_1 and W_2 are the weight losses (mg cm^{-2}) in the presence and absence of the extract, respectively, A is the area of the specimen in cm^{-2} and t is the period of immersion in min.

2.4. Potentiodynamic polarization measurements

Before polarization scanning, working electrode was immersed in the test solution (100 ml) for 30 min until steady state was attained, this was taken as open circuit potential (EOC). All experiments were carried out at 25 ± 1˚C and solutions were not aerated. For polarization measurements, potential from −300 to 100 mV [relative to open circuit potential, (E_{OCP})] was applied. The IE was calculated using Eq. (3):

$$\% \text{ IE} = [1 - (i_{\text{corr(inh)}}/i_{\text{corr(free)}})] \times 100 \quad (3)$$

where $i_{\text{corr(free)}}$ and $i_{\text{corr(inh)}}$ are the corrosion current densities in the absence and presence of extract, respectively.

2.5. Electrochemical impedance spectroscopy (EIS) method

The EIS spectra were recorded at EOC after immersion of the electrode for 30 min in the test solution in order to attain steady state. The AC signal was 5 mV peak to peak and the frequency range studied was between 100 and 0.2 Hz.

The % IE and the surface coverage (θ) of the used inhibitors obtained from the impedance measurements can be calculated using Eq. (4):

$$\% \text{ IE} = \theta \times 100 = [1 - (R^{\circ}_{ct}/R_{ct})] \times 100 \quad (4)$$

R°_{ct} and R_{ct} are the charge transfer resistance in the absence and presence of inhibitor, respectively

2.6. Electrochemical frequency modulation (EFM)

EFM was carried out using two frequencies, 2 and 5 Hz. The base frequency was 0.1 Hz, so the waveform repeats after 1 s. The intermodulation spectra contain current responses assigned for harmonical and intermodulation current peaks. The larger peaks were used to calculate the corrosion current density (i_{corr}), the Tafel slopes (β_c and β_a), and the causality factors CF-2 and CF-3 [36,37].

All electrochemical experiments were carried out using Potentiostat/Galvanostat/Zra analyzer (Gamry PCI300/4). A personal computer with DC 105 software for polarization, EIS 300 software for impedance, EFM140 software for EFM, and Echem Analyst 5.21 was used for data fitting and calculating.

2.7. Quantum chemical calculations

All the quantum chemical calculations were performed with Material Studio semi-empirical program using PM3 method. The following quantum chemical indices were considered: energy of the highest occupied molecular orbital (E_{HOMO}), energy of the lowest unoccupied molecular orbital (E_{LUMO}), $\Delta E = (E_{LUMO}) - (E_{HOMO})$, and dipole moment (μ).

3. Results and discussion

3.1. Weight loss measurements

The weight loss–time curves of 304 SS specimens in 1 M HCl solution, with and without different concentrations, from the investigated fennel seeds extract determined after 3 h of immersion at 25˚C are given in Fig. 2. The % IEs are given in Table 1.The presence of inhibitor reduces the CR of 304 SS in HCl. From the plot, weight loss for systems containing fennel extract

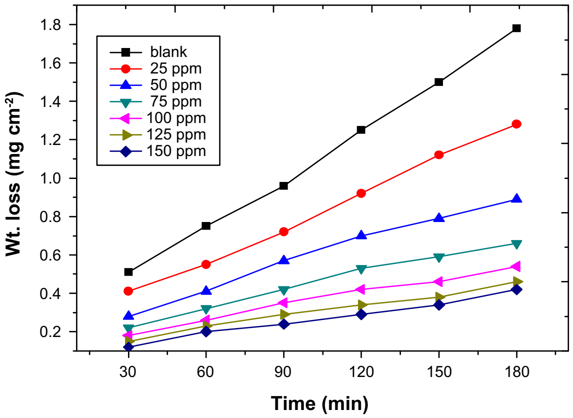

Fig. 2. Weight loss–time curves for the corrosion of 304 SS in 1 M HCl in absence and presence of different concentrations of fennel extract at 25°C.

Table 1
Data of weight loss measurements for 304 SS in 1 M HCl solution in the absence and presence of different concentrations of fennel extract at temperature ranges (25–40°C)

Temperature	Conc. (ppm)	Weight loss (mg/cm²)	θ	% IE
25°C	25	0.670	0.464	46.4
	50	0.623	0.502	50.2
	75	0.485	0.612	61.2
	100	0.414	0.669	66.9
	125	0.339	0.729	72.9
	150	0.285	0.772	77.2
30°C	25	0.73	0.434	43.4
	50	0.68	0.473	47.3
	75	0.54	0.581	58.1
	100	0.47	0.636	63.6
	125	0.4	0.69	69.0
	150	0.34	0.731	73.1
35°C	25	0.8	0.398	39.8
	50	0.75	0.444	44.4
	75	0.62	0.609	60.9
	100	0.55	0.593	59.3
	125	0.47	0.652	65.2
	150	0.42	0.689	68.9
40°C	25	0.93	0.359	35.9
	50	0.88	0.393	39.3
	75	0.74	0.49	49.0
	100	0.66	0.545	54.5
	125	0.58	0.6	60.0
	150	0.54	0.627	62.7

was found to be lower compared with the blank indicating that different concentrations of fennel extract retard the corrosion of 304 SS in 1 M HCl. The Figure reveals that the inhibitor (plant extract) actually inhibited the HCl-induced corrosion of 304 SS to an appreciable extent. The Figure also reveals that 304 SS corrosion by HCl occurs not by simple homogenous process but by a heterogeneous one consisting of different or same rates. This assertion is made from the nonuniformity or nonlinearity of the plots obtained [38]. Table 1 shows the data of weight loss measurements for 304 SS in 1 M HCl solution in the absence and presence of different concentrations of fennel extract at temperature ranges (25–40°C).

3.2. Adsorption isotherm and thermodynamics parameters

The mechanism of the interaction between inhibitor and the metal surface can be explained using adsorption isotherms. The degree of surface coverage, θ, was computed for the different concentrations of the extract from weight loss measurements as follows: $\% \text{ IE} = \theta \times 100$, assuming direct relationship between surface coverage and IE. The surface coverage values obtained were applied to various adsorption isotherm models. By far, the best fit was found to obey Langmuir adsorption isotherm (Fig. 3), which may be formulated as in Eq. (5):

$$C/\theta = 1/K_{\text{ads}} + C \tag{5}$$

where K_{ads} is the adsorption equilibrium constant of the inhibitor, C is the inhibitor concentration, and θ is the surface coverage. The free energy of adsorption ($\Delta G^{\circ}_{\text{ads}}$) can be obtained from Eq. (6):

$$\log K_{\text{ads}} = -\log 55.5 - \Delta G^{\circ}_{\text{ads}}/2.303RT \tag{6}$$

where R is the universal gas constant and T is the absolute temperature; the value 55.5 is the concentration of water on the metal surface in mol/L.

The negative values of $\Delta G^{\circ}_{\text{ads}}$ in Table 2 suggested that the adsorption of inhibitor molecules onto 304 SS surface is a spontaneous process. Generally, values of $\Delta G^{\circ}_{\text{ads}}$ up to $-20\,\text{kJ}\,\text{mol}^{-1}$ are consistent with the electrostatic interaction between the charged molecules and the charged metal (physical adsorption), while those more negative than $-40\,\text{kJ}\,\text{mol}^{-1}$ involve charge sharing or transfer of electrons from the inhibitor molecules to the metal surface to form a co-ordinate type of bond (chemisorption) [39,40]. The large K_{ads} value gives better IE due to strong electrical interaction between the double layer and adsorbing inhibitor molecules, while a small K_{ads} value compromises that

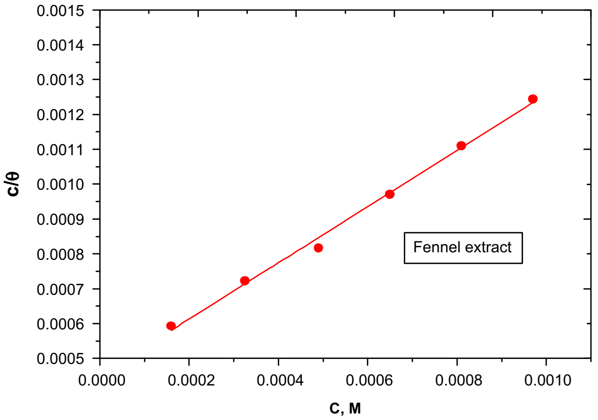

Fig. 3. Adsorption isotherm for the adsorption of extract on 304 SS in 1 M HCl at 25˚C.

such interactions between the adsorbing inhibitor molecules and the metal surface are weaker, indicating that the inhibitor molecules are easily removable by the solvent molecules from the surface of 304 SS. Fig. 4 shows the plot of log K_{ads} vs. $1/T$, a straight line with an intercept equal to ΔH°_{ads} with slope equal to ΔS°_{ads} in Eq. (7):

$$\Delta G^{\circ}_{ads} = \Delta H^{\circ}_{ads} - T\Delta S^{\circ}_{ads} \tag{7}$$

The negative sign of ΔH°_{ads} indicated that the adsorption of inhibitor molecules is an exothermic process in all cases. The sign of ΔS°_{ads} is negative because inhibitor molecules freely moving in the bulk solution were adsorbed in an orderly fashion on to 304 SS resulting in a decrease in entropy [41]. Moreover, from thermodynamic principles, since the adsorption was an exothermic process, it must be accompanied by a decrease in entropy [42].

3.3. Effect of temperature

Temperature plays an important role on metal dissolution. The CR in acid solution, for example, increases exponentially with temperature increase because the hydrogen evolution overpotential increases [43]. In order to access the effect of temperature on the corrosion and corrosion inhibition process, weight loss experiments were carried out in the temperature range 25–40˚C in 1 M HCl in the absence and presence of different concentrations (25–150 ppm) of fennel extract. It was found that after 3 h immersion period, the surface coverage and IE decrease with rise in temperature (Table 1). Arrhenius-type dependence is observed between CR and temperature often expressed as in Eq. (8):

$$\text{Corrosion Rate (CR)} = A\exp -E^{*}_{a}/RT \tag{8}$$

where CR is the corrosion rate, E^{*}_{a} is the apparent activation energy, R is the molar gas constant, T is the absolute temperature, and A is the frequency factor.

Fig. 5 depicts an Arrhenius plot (logarithm of CR against the reciprocal of temperature ($1/T$)) for 304 SS in 1 M HCl solution in the absence and presence of different extract concentrations. Satisfactory straight lines of high correlation coefficients were obtained. The values of activation energy were obtained from the slopes of the linear plots and are given in Table 3. It is clear that E^{*}values in the presence of the different concentrations of the extract are higher than in their absence. The higher value in apparent activation energy in the presence of the extract denotes physical adsorption, while the reverse is usually attributed to chemical adsorption [44]. This conclusion is denoted by the decrease in IE with increasing temperature (Table 1). Similar result has been reported by Okafor et al. [45] on the inhibition of acid corrosion of carbon steel using aqueous extract of *P. amarus* seeds and leaves. Moreover, the increase in activation energy is proportional to the inhibitor concentration indicating that the energy barrier for the corrosion process is also increased [46]. An alternative formulation of Arrhenius equation is [47]:

$$CR = (RT/Nh)\exp(\Delta S^{*}/R)\exp(-\Delta H^{*}/RT) \tag{9}$$

where h is the Planck's constant, N is the Avogadro's number, ΔS^{*} is the entropy of activation, and ΔH^{*} is the enthalpy of activation.

Fig. 6 shows a plot of Log (CR/T) as a function of $1/T$. Straight lines were obtained with a slope of ($\Delta H^{*}/R$) and an intercept of ($\ln R/Nh - \Delta S^{*}/RT$) from which the values of ΔH^{*} and ΔS^{*} were calculated (Table 3). The positive values of ΔH^{*} both in the absence and presence of the extract reflect the endothermic nature of the 304 SS dissolution process. It is also clear that the activation enthalpies vary in the

Table 2
Thermodynamic parameters for 304 SS in 1 M HCl for fennel seeds extract

Inhibitor	Temp. (K)	$-\Delta S^{\circ}_{ads}$ (J mol^{-1} K^{-1})	$-\Delta H^{\circ}_{ads}$ (kJ mol^{-1})	$-\Delta G^{\circ}_{ads}$ (kJ mol^{-1})	K_{ads} (M^{-1})
Extract	298	10.7	25.8	29.0	2,210

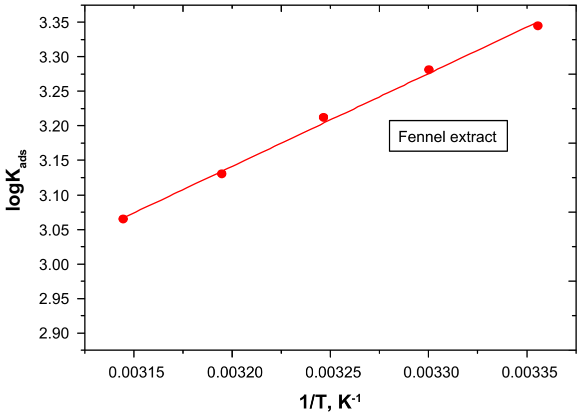

Fig. 4. Variation of log K$_{ads}$ with $1/T$.

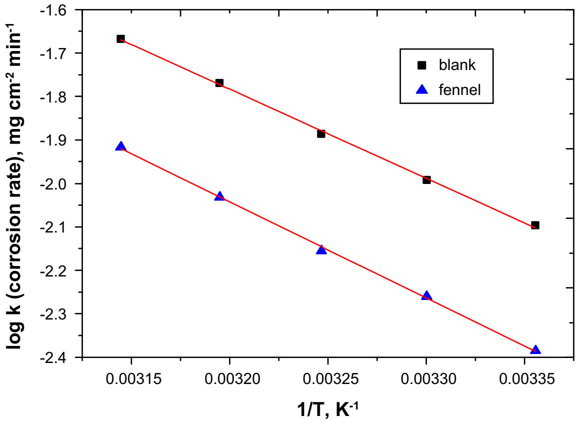

Fig. 5. Arrhenius plot of variation of (log K) vs. (1/T) for dissolution of 304 SS in 1 M HCl in in absence and presence of 50 ppm of fennel extract.

same manner as the activation energies, supporting the proposed inhibition mechanism. Large and negative values of entropies imply that the activated complex in the rate-determining step represents an association rather than a dissociation step, meaning that a decrease in disordering takes place on going from reactants to the activated complex. Similar observation has been reported in the literature [45].

3.4. Potentiodynamic polarization measurements

Potentiodynamic polarization curves for 304 SS in uninhibited and inhibited acidic solutions containing different concentrations of fennel extract are shown in Fig. 7. The corrosion kinetic parameters derived from potentiodynamic polarization curves together with % IE are listed in Table 4. It has been observed that values of corrosion current density (i_{corr}) for 304 SS in 1 M HCl solution decreased with increase in fennel extract concentration. The decrease in corrosion current densities in the presence of inhibitor might be due to the adsorption of fennel extract component molecules on the 304 SS surface. In the absence and presence of fennel extract, β_a and β_c values remain more or less identical indicating that the effect of extract is not as large as to change the mechanism of corrosion. The value of corrosion potential ($E_{corr.}$) showed a slight shift towards anodic region as the concentration of extract increased, suggesting that the effect of extract is more pronounced at anodic site. It was reported before [48] that, if the displacement in corrosion potential is more than 85 mV with respect to corrosion potential of uninhibited solution, the inhibitor can be seen as a cathodic or anodic type. In our study, the maximum displacement was 15 mV, indicating that fennel extract belonged to mixed type.

3.5. EIS

The corrosion of 304 SS in 1 M HCl in the presence of fennel extract was investigated by EIS method at 25˚C. Impedance parameters, such as charge transfer resistance R_{ct}, which is equivalent to R_p, and the double-layer capacitance C_{dl}, are derived from the Nyquist plot (Fig. 8) and are given in Table 5 for 304 SS in 1 M HCl acid solution in the presence and absence of the extract. It is observed that the values of R_{ct} increase with increasing the concentration of the extract and this in turn leads to a decrease in CR of 304 SS in 1 M HCl acid solution. Impedance diagram has a semicircular appearance; the diagram indicates that the corrosion of 304 SS is mainly controlled by a charge transfer process [49]. The values of double-layer capacitance, C_{dl}, decrease with increasing

Table 3
Kinetic activation parameters for 304 SS in 1 M HCl in the absence and presence 50 ppm fennel extract

Inhibitors	Conc. (ppm)	Activation parameters		
		E_a^* (kJ mol^{-1})	ΔH^* (kJ mol^{-1})	$-\Delta S^*$ (J mol^{-1}K^{-1})
Blank	0.0	39.2	36.7	162.1
Extract	50	42.3	39.2	158.0

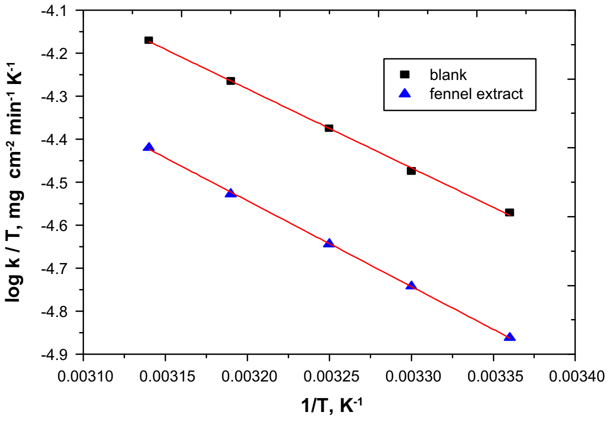

Fig. 6. Arrhenius plot of variation of (log CR/T) vs. (1/T) for dissolution of 304 SS in 1 M HCl in in absence and presence of 50 ppm of fennel extract.

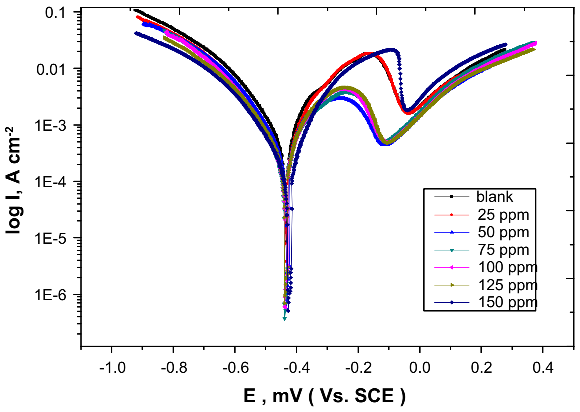

Fig. 7. Potentiodynamic polarization curves of 304 SS in 1 M HCl in the absence and presence of different concentrations of fennel extract at 25˚C.

concentration of fennel extract. A low capacitance may result if water molecules at the electrode interface are replaced by inhibitor molecules of lower dielectric constant through adsorption. When such low capacitance values are in connection with high R_{ct} values, it is apparent that a relationship exists between adsorption and inhibition.

The impedance data of 304 SS in 1 M HCl are analyzed in terms of an equivalent circuit model (Fig. 9) which includes the solution resistance R_s and double-layer capacitance C_{dl} that is placed in parallel to the charge transfer resistance R_{ct} [50] due to charge transfer reaction. C_{dl} can be calculated from the angular frequency ($\omega = 2\pi f$) at the maximum imaginary component and the charge transfer resistance according Eq. (10):

$$C_{d1} = [1/\omega_{max} R_p] = [1/2\pi f_{max} R_p] \qquad (10)$$

where f is maximum frequency, ω is the angular velocity

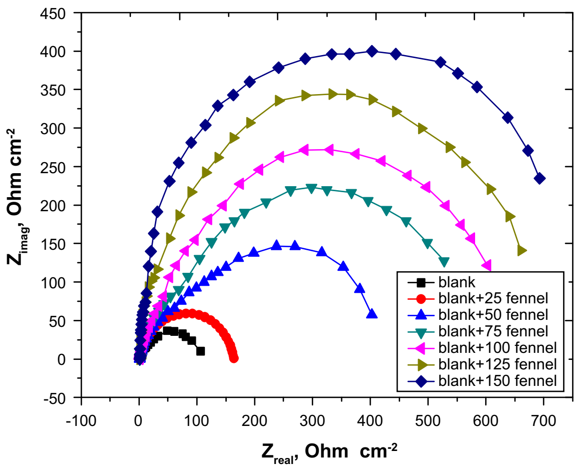

Fig. 8. Nyquist plot of 304SS in 1 M HCl in the absence and presence of different concentrations of fennel extract at 25˚C.

Table 4
Corrosion parameters obtained from potentiodynamic polarization of 304SS in 1 M HCl containing various concentrations of fennel extract at 25 ˚C

Comp.	Conc. (ppm)	$-E_{corr}$ (mV) vs. SCE	i_{corr} (mA cm^{-2})	β_c (mV dec^{-1})	β_a (mV dec^{-1})	θ	% IE	CR (mm y^{-1})
Blank	0.0	444	493.0	215.0	195.3	–	–	5.022
Extract	25	440	253.4	210.3	187.2	0.486	48.6	2.581
	50	439	205.1	6.208	182.4	0.584	58.4	2.089
	75	435	149.8	207.4	177.6	0.696	69.6	1.526
	100	431	129.2	203.9	173.9	0.738	73.8	1.316
	125	430	95.60	199.8	168.3	0.806	80.6	0.974
	150	429	70.00	195.7	165.8	0.858	85.8	0.713

Table 5
EIS data of 304 SS in 1 M HCl and in the presence and absence of different concentrations of fennel extract at 25˚C

Comp.	Conc. (ppm)	R_S (Ω cm^2)	C_{dl} (μF cm^{-2})	n	R_{ct} (Ω cm^2)	θ	% IE_{EIS}
Blank	0.0	1.321	30.597	0.834	89.2	–	–
Extract	25	1.242	25.169	0.862	150.9	0.409	40.9
	50	1.164	22.378	0.853	350.4	0.745	74.5
	75	1.152	20.172	0.814	480.9	0.815	81.5
	100	1.121	18.161	0.846	530.3	832.0	83.2
	125	1.117	16.361	0.881	615.9	0.855	85.5
	150	1.110	14.931	0.873	700.2	0.873	87.3

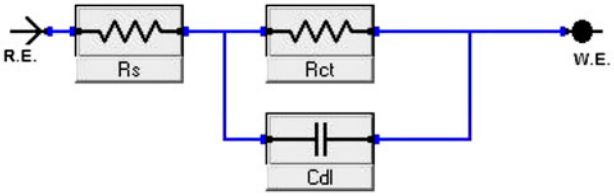

Fig. 9. Equivalent circuit model used to fit impedance data.

3.6. EFM

The EFM is a nondestructive corrosion measurement technique that can directly give values of the corrosion current without prior knowledge of Tafel constants. Like EIS, it is a small ac signal. Intermodulation spectra obtained from EFM measurements are presented in Fig. 10 for 1 M HCl in the absence and presence of different concentrations of fennel extract at 25˚C. Each spectrum is a current response as a function of frequency. The calculated corrosion kinetic parameters at different concentrations of fennel extract in 1 M HCl at 25˚C (i_{corr}, β_a, β_c, CF-2, CF-3, and % IE) are given in Table 6. From Table 6, the corrosion current densities decrease by increasing the concentration of fennel extract and the IE increases by increasing the extract concentration. The causality factors in Table 6 are very close to theoretical values (2.0 and 3.0) which according to EFM theory should guarantee the validity of Tafel slopes and corrosion current densities and indicate that the measured data are of good quality. The deviation of causality factors from their ideal values might be due to the reason that perturbation amplitude was too small or the resolution of the frequency spectrum is not high enough. Also, another possible explanation is that the inhibitor is not performing very well. The obtained results showed good agreement of IE obtained from the potentiodynamic polarization, EIS, and weight loss methods.

3.7. Quantum chemical calculations

Fig. 11 shows the optimized structures of the fennel extract. Quantum structure–activity relationships have been used to study the effect of molecular structure on IE of the investigated inhibitor. Table 7 shows the quantum chemical calculation parameters (E_{HUMO}, E_{LUMO}) and the energy band gap ($\Delta E = E_{HUMO} - E_{LUMO}$) is also listed. E_{HUMO} is often associated with the electron-donating ability of the molecule. High E_{HUMO} values indicate that the molecule has a tendency to donate electrons to appropriate acceptor molecules with low-energy empty molecular orbital. Increasing values of the E_{HUMO} facilitate adsorption (and therefore, inhibition) by influencing the transport process through the adsorbed layer [51,52]. E_{LUMO} indicates the ability of the molecules to accept electrons. The lower values of the E_{LUMO}, the more probable it is that the molecule would accept electrons [51,52]. Low absolute values of the energy band gap (ΔE) gives good inhibition efficiencies because the energy to remove an electron from the last occupied orbital will be low. This is a good agreement with the previously mentioned experimental data obtained by weight loss, potentiodynamic polarization, and EIS techniques.

3.8. Mechanism of corrosion inhibition

The isotherm depicted in Fig. 3 characterizes the spontaneous physisorption of phytochemicals composition (Table 1) of fennel seeds extract on heterogeneous surfaces [53]. Thus, the mechanism of corrosion inhibition of 304 SS in acidic solution by the phytochemicals of the extract can be explained on the basis of adsorption on the metal surface. This indicates that the IE of the extract is due to the presence of some or all the above listed phytochemical constituents. The adsorption of the inhibitor molecules on the 304 SS surface is due to the donor—acceptor interaction between π electrons of donor atoms O and aromatic

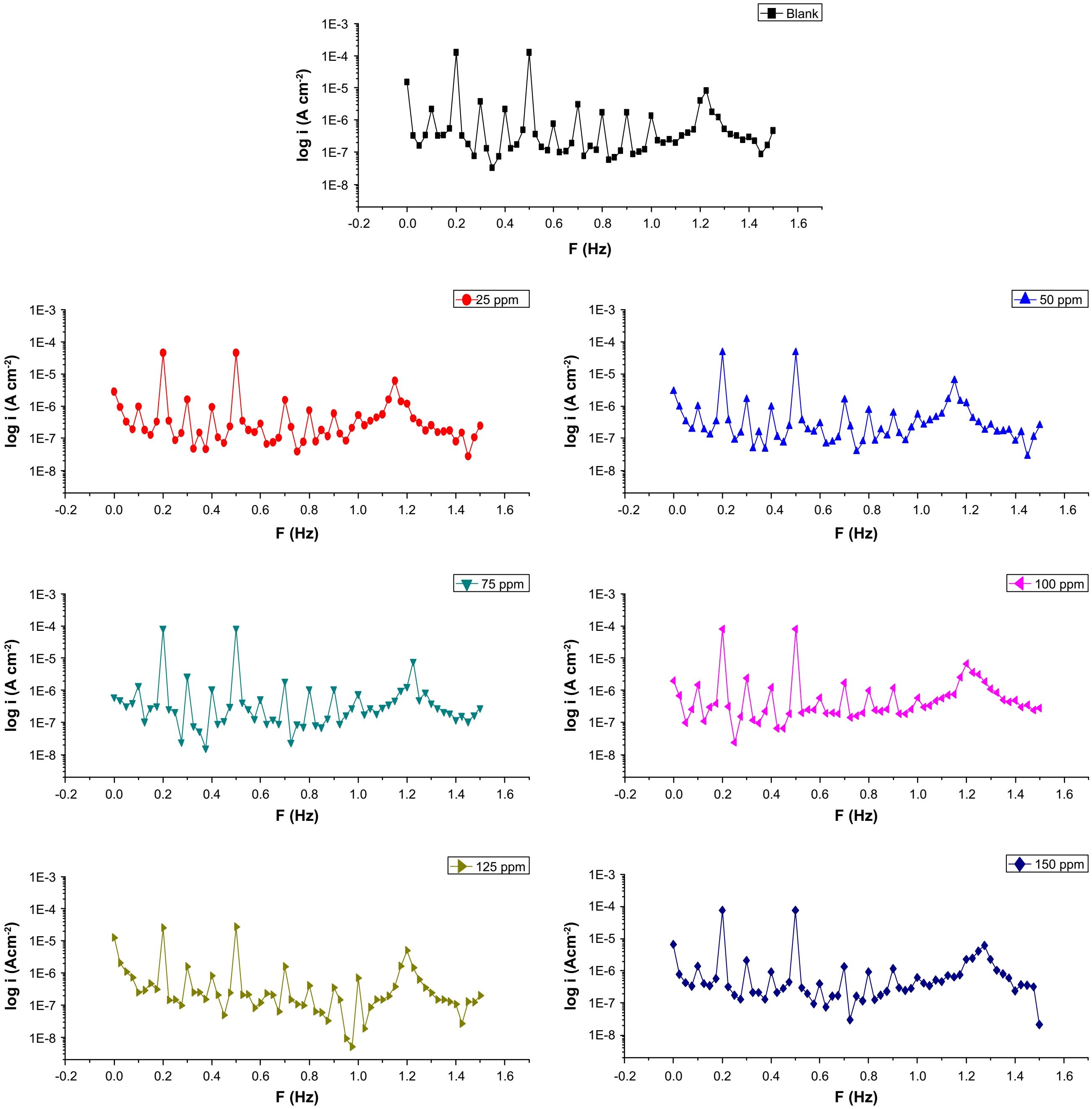

Fig. 10. EFM spectra for 304 SS in 1 M HCl solutions in the presence and absence of different concentrations of fennel extract at 25˚C.

rings of inhibitors and the acceptor, i.e. vacant d orbital of iron surface atoms [54]. The inhibitor molecules can also be adsorbed on the metal surface in the form of negatively charged species which can interact electrostatically with positively charged metal surface, which led to increase the surface coverage and consequently protect efficiency even in the case of low inhibitor concentration. Eddy and Ebenso [55] also stated that sapponins, tannins, and alkaloids are active constituents of most green inhibitors.

Table 6
Electrochemical kinetic parameters obtained from EFM technique for 304 SS in the absence and presence of various concentrations of fennel extract in 1 M HCl at 25˚C

Comp.	Conc. (ppm)	i_{corr} (μAcm^{-2})	β_c (mVdec^{-1})	β_a (mVdec^{-1})	CF-2	CF-3	θ	% IE	CR (mmy^{-1})
Blank	00	5330.5	233.3	211.6	1.782	2.811	–	–	7.216
Extract	25	2648.7	228.4	208.4	1.643	2.641	0.503	50.3	3.541
	50	1982.4	220.1	203.6	1.821	2.501	0.628	62.8	2.684
	75	1519.7	217.6	196.3	1.511	2.716	0.715	71.5	2.054
	100	1321.4	209.1	182.5	1.881	2.820	0.752	75.2	1.789
	125	895.0	198.3	176.9	1.943	2.900	0.832	83.2	1.212
	150	687.1	187.4	166.4	1.660	2.898	0.871	87.1	0.930

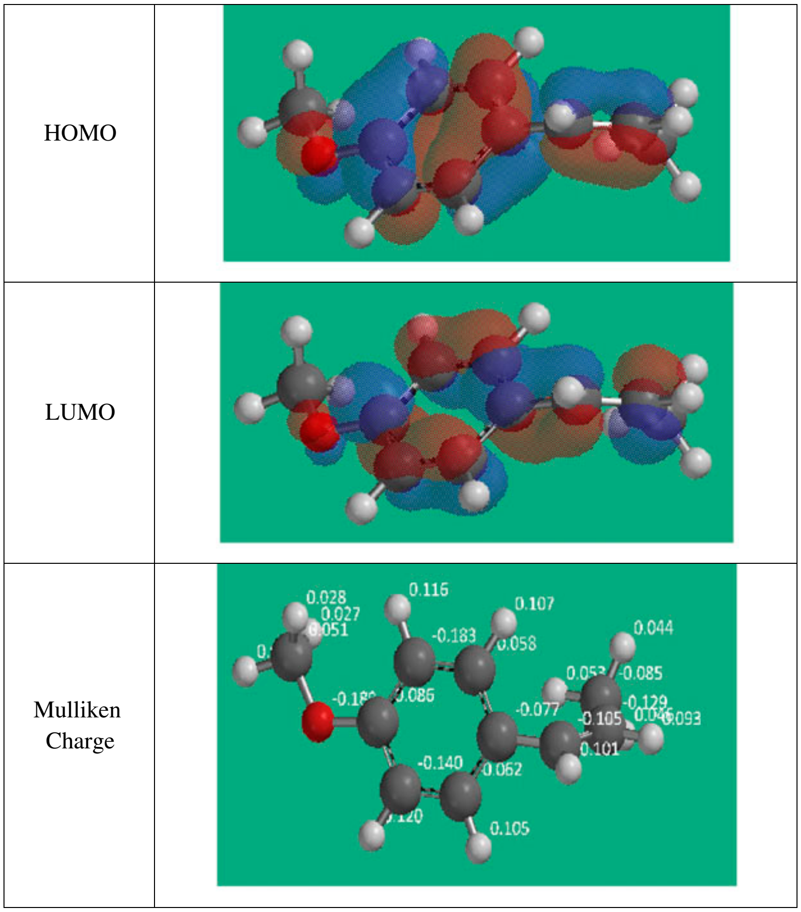

Fig. 11. HOMO, LUMO structures and Mulliken charge of fennel extract.

Table 7
Calculated quantum chemical parameters for fennel extract (Anethol) using PM3

PM3 liquidphase	E_{HOMO} (eV)	E_{LUMO} (eV)	ΔE (eV)	μ (debyes)
Extract (anethol)	−8.83	0.22	8.61	1.54

4. Conclusions

Based on the above results, the following conclusions can be drawn:

- Aqueous extract of fennel seeds extract was found to be an efficient inhibitor for the corrosion of 304 SS in 1 M HCl
- IE increased with an increase in fennel seeds extract content in 1 M HCl but decreased with rise in temperature
- The corrosion process is inhibited by adsorption of the fennel seeds extract on the 304 SS surface following Langmuir adsorption isotherm. This indicates that the inhibition effect of the extract is due to adsorption of some or all the listed phytochemical constituents
- Adsorption of aqueous extract of fennel seeds extract on the surface of the 304 SS is spontaneous and occurs by physical adsorption
- The negative free energy $(-\Delta G^{\circ}_{\mathrm{ads}})$ of adsorption indicates strong and spontaneous adsorption of the fennel seeds extract on the 304 SS surface
- Values of Tafel constants β_a and β_c confirm that the fennel seeds extract acts like mixed type inhibitor
- Increase in R_p and R_{ct} values and decrease in i_{corr} and C_{dl} values confirm that the fennel seeds extract is adsorbed on the mild steel surface and inhibition process is followed by monolayer adsorption
- The inhibition efficiencies determined by mass loss and electrochemical methods are in reasonable good agreement
- Thus, the fennel seeds extract was proved to be an effective eco-friendly and low-cost inhibitor.

References

[1] M. Abdallah, Rhodanine azosulpha drugs as corrosion inhibitors for corrosion of 304 stainless steel in hydrochloric acid solution, Corros. Sci. 44 (2002) 717–728.

[2] M. Abdallah, Guar gum as corrosion inhibitor for carbon steel in sulfuric acid solutions, Port. Electrochim. Acta 22 (2004) 161–175.

[3] M. Abdallah, Antibacterial drugs as corrosion inhibitors for corrosion of aluminum in hydrochloric solution, Corros. Sci. 46 (2004) 1981–1996.

[4] Y.K. Agrawal, J.D. Talati, M.D. Shah, M.N. Desai, N.K. Shah, Schiff bases of ethylenediamine as corrosion inhibitors of zinc in sulphuric acid, Corros. Sci. 46 (2003) 633–651.

[5] P. Arora, S. Kumar, M.K. Sharma, S.P. Mathur, Corrosion inhibition of aluminum by *Capparis decidua* in acidic media, E. J. Chem. 4(4) (2007) 450–456.

[6] M.I. Awad, Eco friendly corrosion inhibitors: inhibitive action of quinine for corrosion of low carbon steel in 1 m HCl, J. Appl. Electrochem. 36 (2006) 1163–1168.

[7] H. Ashassi-Sorkhabi, N. Ghalebsaz-Jeddi, Inhibition effect of polyethylene glycol on the corrosion of carbon steel in sulphuric acid, Mater. Chem. Phys. 92 (2005) 480–486.

[8] H. Ashassi-sorkhabi, B. Shaabani, B. Aligholipour, D. Seifzadeh, The effect of some Schiff bases on the corrosion of aluminum in hydrochloric acid solution, Appl. Surf. Sci. 252 (2006) 4039–4047.

[9] M. Gopiraman, P. Sakunthala, D. Kesavan, V. Alexramani, I.S. Kim, N. Sulochana, An investigation of mild carbon steel corrosion inhibition in hydrochloric acid medium by environment friendly green inhibitors, J. Coat. Technol. Res. 9(1) (2012) 15–26.

[10] M.N. Lavanya, D. Kesavan, N. Prabhavathi, N. Sulochana, Studies on inhibitive effect of 3-hydroxyflavone on the acid corrosion of mild steel, Surf Rev Lett. 16 (2009) 845–853.

[11] M. Gopiraman, C. Sathya, S. Vivekananthan, D. Kesavan, N. Sulochana, Influence of 2,3-dihydroxyflavanone on corrosion inhibition of mild steel in acidic medium, J. Mater. Eng. Perform. 21 (2012) 240–246.

[12] S. Ashok Kumar, M. Gopiraman, M. Saravana Kumar, A. Sreekanth, 2-Acetylpyridine *N*(4) morpholine thiosemicarbazone (HAcpMTSc) as a corrosion inhibitor on mild steel in HCl, Ind. Eng. Chem. Res. 50 (2011) 7824–7832.

[13] M. Gopiraman, N. Selvakumaran, D. Kesavan, R. Karvembu, Adsorption and corrosion inhibition behavior of *N*-(phenylcarbamothioyl) benzamide on mild steel in acidic medium, Prog. Org Coat. 73 (2012) 104–111.

[14] D. Kesavan, M. Muthu Tamizh, M. Gopiraman, N. Sulochana, R. Karvembu, Physicochemical studies of 4-substitute *N*-(2-mercaptophenyl)-salicylideneimines: corrosion inhibition of mild steel in an acid medium, J. Surfact. Deterg. 15(5) (2012) 567–576. doi: 10.1007/s11743-012-1338-z

[15] R. Baskar, M. Gopiraman, D. Kesavan, I.S. Kim, K. Subramanian, Synthesis, characterization, and electrochemical studies of novel biphenyl based compounds, Ind. Eng. Chem. Res. 15 (10) (2012) 3966–3974. doi: 10.1021/ie201470j

[16] D. Kesavan, M. Gopiraman, N. Sulochana, Green inhibitors for corrosion of metals: a review, Chem. Sci. Rev. Lett. 1(1) (2012) 1–8.

[17] C.A. Loto, The effect of mango bark and leaf extract solution additives on the corrosion inhibition of mild steel in dilute sulphuric acid. Part 1, Corros. Prev. Cont. 48 (2001) 38–41.

[18] C.A. Loto, The effect of mango bark and leaf extract solution additives on the corrosion inhibition of mild steel in dilute sulphuric acid. Part 2, Corros. Prev. Cont. 48 (2001) 59–64.

[19] G. Gunasekaran, L.R. Chauhan, Eco friendly inhibitor for corrosion inhibition of mild steel in phosphoric acid medium, Electrochim. Acta 49 (2004) 4387–4395.

[20] A.K. Satapathy, G. Gunasekaran, S.C. Sahoo, A. Kumar, P.V. Rodrigues, Corrosion inhibition by *Justicia gendarussa* plant extract in hydrochloric acid/solution, Corros. Sci. 51 (2009) 2848–2856.

[21] P.C. Okafor, M.E. Ikpi, I.E. Uwah, E.E. Ebenso, U.J. Ekpe, S.A. Umoren, Inhibitory action of *Phyllanthus amarus* extracts on the corrosion of mild steel in acidic media, Corros. Sci. 50 (2008) 2310–2317.

[22] A. Bouyanzer, B. Hammouti, L. Majidi, Pennyroayl oil from *Mentha pulegium* as corrosion inhibitor for steel in 1 M HCl, Mater. Lett. 60 (2006) 2840–2843.

[23] L. Majidi, M. Idrissi, M. Hnach, Biosynthesis, synthesis, and reactivity of R-(+)-Pulegone: principal constituent of the essential oil of pennyroyal mint (*Mentha pulegium*), Chem. Inform. 36 (2005) 657–670. doi: 10.1002/chin.200514273

[24] O.L. Riggs, Corrosion inhibitors, 2nd ed., Nathan CC, Houston, TX, p. 43 1973.

[25] A. Chetouani, B. Hammouti, M. Benkaddour, Corrosion inhibition of iron in hydrochloric acid solution by jojoba oil, Pigm. Res. Technol. 33 (2004) 26–31.

[26] A. Bouyanzer, B. Hammouti, A study of anti-corrosive effects of Artemisia oil on steel, Pigm. Res. Technol. 33 (2004) 287–292.

[27] P. Bothi Raja, M.G. Sethuraman, Inhibitive effect of black pepper extract on the sulphuric acid corrosion of mild steel, Mater Lett. 62 (2008) 2977–2979.

[28] M.G. Sethuraman, P. Bothi Raja, Corrosion inhibition of mild steel by Datura metel, Pigm. Res. Technol. 34 (2005) 327–331.

[29] P. Bothi Raja, M.G. Sethuraman, *Strychnos nux-vomica* an eco-friendly corrosion inhibitor for mild steel in 1 M sulfuric acid medium, Mater. Corros. 60 (2009) 22–28.

[30] A.Y. El-Etre, Khilah extract as inhibitor for acid corrosion of SX 316 steel, Appl. Surf. Sci. 252 (2006) 8521–8525.

[31] A.M. Abdel-Gaber, B.A. Abd-El-Nabey, M. Saadawy, The role of acid anion on the inhibition of the acidic corrosion of steel by lupine extract, Corros. Sci. 51 (2009) 1038–1042.

[32] P.C. Okafor, E.E. Ebenso, Inhibitive action of Carica papaya extracts on the corrosion of mild steel in acidic media and their adsorption characteristics, Pigm. Res. Technol. 36 (2007) 134–140.

[33] A.Y. El-Etre, Inhibition of C-steel corrosion in acidic solution using the aqueous extract of zallouh root, Mater. Chem. Phys. 108 (2008) 278–282.

[34] W. Aneta, O. Jan, C. Renata, Antioxidant activity and phenolic compounds in 32 selected herbs, Food Chem. 105 (2007) 940–949.

[35] J.D. Talati, R.M. Modi, Inhibition of corrosion of aluminum–copper alloy in sodium hydroxide, Trans. SEAST 11 (1986) 259–271.

[36] S.S. Abdel-Rehim, K.F. Khaled, N.S. Abd-Elshafi, Electrochemical frequency modulation as a new technique for monitoring corrosion inhibition of iron in acid media by new thiourea derivative, Electrochim. Acta 51 (2006) 3269–3277.

[37] R.W. Bosch, J. Hubrecht, W.F. Bogaerts, B.C. Syrett, Electrochemical technique for online corrosion monitoring corrosion 57 (2001) 60–70.

[38] N. Lahhit, A. Bouyanzer, J.-M. Desjobert et al., Fennel (*Foeniculum vulgare*) essential oil as green corrosion inhibitor of stainless steel in hydrochloric acid solution, Port. Electrochim. Acta 29(2) (2011) 127–138.

[39] F.M. Donahue, K. Nobe, Theory of organic corrosion inhibitors: adsorption and linear free energy relationships, J. Electrochem. Soc. 112 (1965) 886–891.

[40] E. Kamis, F. Belluci, R.M. Latanision, E.S.H. El-Ashry, Acid corrosion inhibition of nickel by 2-(triphenosphoranylidene) succinic anhydride, Corrosion 47 (1991) 677–686.

[41] X. Li, G. Mu, Tween-40 as corrosion inhibitor for cold rolled steel in sulphuric acid: Weight loss study, electrochemical characterization, and AFM, Appl. Surf. Sci. 252 (2005) 1254–1265.

[42] G. Mu, X. Li, G. Li, Synergistic inhibition between tween 60 and NaCl on the corrosion of cold rolled steel in 0.5 M sulfuric acid, Corros. Sci. 47 (2005) 1932–1952.

[43] F.S. de Souza, A. Spinelli, Caffeic acid as a green corrosion inhibitor for mild steel, Corros. Sci. 51 (2009) 642–649.

[44] M.I. Awad, Eco friendly corrosion inhibitors: inhibitive action of quinine for corrosion of low carbon steel in 1 M HCl, J. Appl. Electrochem. 36 (2006) 1163–1168.

[45] P.C. Okafor, M.E. Ikpi, I.E. Uwah, E.E. Ebenso, U.J. Ekpe, S. A. Umoren, Inhibitory action of *Phyllanthus amarus* extracts on the corrosion of mild steel in acidic media, Corros. Sci. 50 (2008) 2310–2317.

[46] A. Popova, E. Sokolova, S. Raicheva, M. Christov, AC and DC study of the temperature effect on mild steel corrosion in acid media in the presence of benzimidazole derivatives, Corros. Sci. 45 (2003) 33–58.

[47] A.S. Fouda, A.A. Al-Sarawy, F.S. Ahmed, H.M. El-Abbasy, Corrosion inhibition of aluminum 6063 using some pharmaceutical compounds, Corros. Sci. 51 (2009) 485–492.

[48] E.S. Ferreira, C. Giancomrlli, F.C. Giancomrlli, A. Spinelli, Evaluation of the inhibitor effect of l-ascorbic acid on the corrosion of mild steel, Mater. Chem. Phys. 83 (2004) 129–134.

[49] M.A. Quraishi, J. Rawad, M. Ajmal, Macrocyclic compounds as corrosion inhibitors corrosion 54 (1998) 996–1002.

[50] J.N. Wanklyn, The role of molybdenum in the crevice corrosion of stainless steels, Corros. Sci. 21 (1981) 211–225.

[51] F.P.A. Robinson, C. Ringas, Corrosion of stainless steel by sulfate-reducing bacteria total immersion test results, Corrosion 44 (1988) 664–671.

[52] W.R. Ciesak, D.J. Duquette, An electrochemical study of the pit initiation resistance of ferritic stainless steels, J. Electrochem. Soc. 132 (1985) 533–538.

[53] E. McCafferty, N. Hackerman, Double layer capacitance of iron and corrosion inhibition with polymethylene diamines, J. Electrochem. Soc. 119 (1972) 146–154.

[54] M. Stern, A.L. Geary, Electrochemical polarization: I. A theoretical analysis of the shape of polarization curves, J. Electrochem. Soc. 104 (1957) 56–63.

[55] N.O. Eddy, E.E. Ebenso, Sapientum peels as a green corrosion inhibitor for mild steel in H_2SO_4, Afri. J. Pure Appl. Chem. 2 (2008) 46–54.